Design and Construction of Continuous Alternate Wheels for an Omnidirectional Mobile Robot

Kyung-Seok Byun and Jae-Bok Song*
Department of Mechanical Engineering
Korea University
5 Anam-dong Sungbuk-gu
Seoul, 136-701, Korea (South)
e-mail: jbsong@korea.ac.kr

Received 1 February 2002; accepted 23 April 2003

Many types of omnidirectional wheels with passive rollers have gaps between rollers. Since these gaps cause a wheel to make discontinuous contact with the ground, they lead to vertical and/or horizontal vibrations during wheel operation. In addition, the radii of passive rollers are related to the height of a bump an omnidirectional wheel can surmount. In this research a new design of the alternate wheel is proposed. Because this wheel makes continuous contact with the ground and has alternating large and small rollers around the wheel, it is termed a continuous alternate wheel (CAW). In this paper a design procedure is also presented to determine the optimum number of rollers, the radii of rollers and the inside inclination angle of an outer roller for given design specifications. The CAW based on this design is compared to the existing alternate wheels in terms of design. Finally, an actual continuous alternate wheel is constructed to verify validity of the design guidelines.

1. INTRODUCTION

Applications of wheeled mobile robots have recently extended to service robots for the handicapped or the aged and industrial mobile robots working in various environments. The most popular wheeled mobile robots are equipped with two independent driving wheels. Since these robots possess 2 degrees-of-motion (DOFs), they can rotate about any point, but cannot perform sideways motion. To overcome this type of limitation on motion, mobile robots with steerable wheels were suggested. They allow both rotation and sideways motions but not simultaneously. If such robots are used as a service robot, for example, they may get in the way of persons they assist, and require unnecessarily large space or move along a complicated path when changing their direction. To cope with these problems, omnidirectional mobile robots were proposed. They are capable of arbitrary

*To whom correspondence should be addressed.
Contract grant sponsor: Korean Research Foundation
Contract grant number: KRF-2002-041-D00038

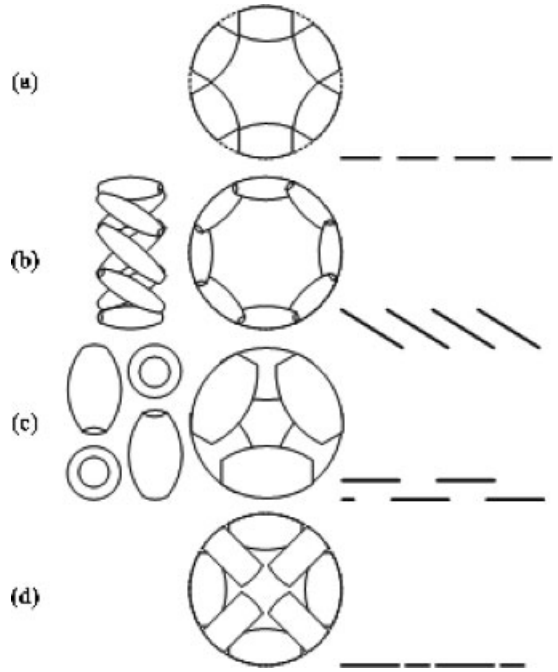

Figure 1. Various wheel types using passive rollers and their traces; (a) classic, (b) Mecanum, (c) double, and (d) alternate.

motion in an arbitrary direction without changing wheel directions, because they can achieve 3 DOF motion on a two-dimensional plane. Various types of omnidirectional mobile robots have been proposed so far; off-centered wheels,[1] ball wheels,[2] and universal wheels[3] are more popular among them.

The initial universal wheel design illustrated in Figure 1(a) has multiple passive rollers whose axes are positioned tangent to the wheel circumference. Since this type of wheel makes discontinuous contact with the ground due to gaps between successive rollers, however, the robot platform suffers from vertical vibrations to some extent. To minimize a gap between rollers, various variations of universal wheels have been devised. In the Mecanum wheel[4] shown in Figure 1(b), rollers are arranged in such a way that contact between the wheel and the ground is continuous. In the double wheels[5] shown in Figure 1(c), wheels are arranged in an overlapping way. These types of wheels touch the ground continuously, but the points of contact with the ground are not continuous as seen in the figures. This discontinuous contact may cause horizontal vibrations.[6] The alternate wheel mechanism[7,8] in Figure 1(d) is another attempt to minimize a gap between rollers for reduction in horizontal and vertical vibrations. Contact points are in line, thus causing little horizontal vibration.

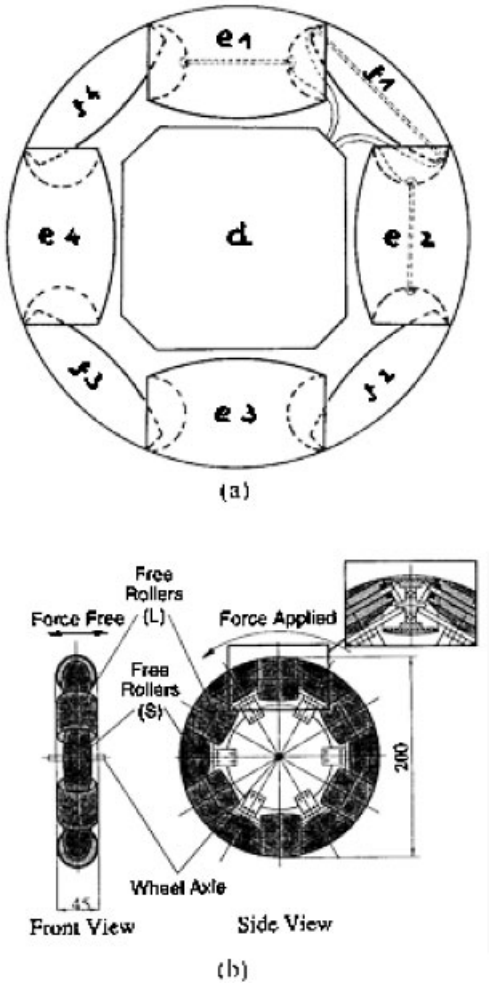

Figure 2. Various alternate wheels; (a) Fuchs and (b) Asama.

Figure 2 shows two types of alternate wheels in which large and small rollers (e.g., 8 rollers[7] and 12 rollers[8]) are alternated to reduce the gap size. Although many different alternate wheels have been designed so far, no systematic design guidelines for the number of rollers and the radii of rollers have been provided. These are important design factors in that the former is related to fabrication cost and the latter to the height of a surmountable bump.

In this research a new design of the alternate wheel is proposed to make the most of good features of alternate wheels. Because the proposed wheel makes continuous contact with the ground and has alternating large and small rollers around the wheel, it will be termed a "continuous alternate wheel (CAW)." This wheel has virtually no gap between rollers as shown in Figure 1 and thus its footprint is

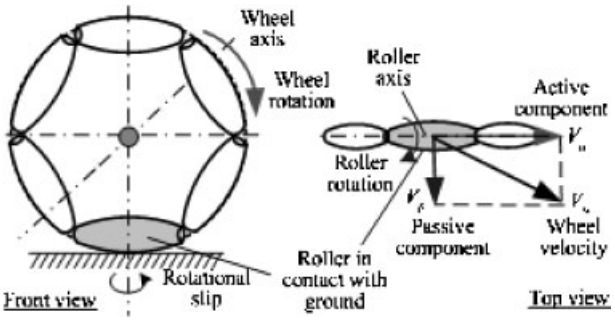

Figure 3. Three DOFs in a general omnidirectional wheel.

continuous unlike some wheels shown in Figures 1 and 2. Since a gap between rollers causes vertical and/or horizontal vibrations in many types of omnidirectional wheels with passive rollers, this feature of no gap (or negligibly small gap) is important in reduction of vibration during the wheel operation. In addition, the radii of rollers can be increased in this wheel, which enables the wheel to surmount a higher bump. This wheel is an improved version of conventional alternate wheels in which inner and outer rollers are disposed alternately.

This paper presents details in the design procedure and construction of CAW. Section 2 briefly introduces the operational principle of CAW and an omnidirectional mobile robot with CAWs. Section 3 deals with various design issues such as the optimum number of rollers and the shape and size of rollers. Section 4 is concerned with the overall structure and construction of the proposed continuous alternate wheel. Conclusions are drawn in Section 5.

2. OPERATION OF OMNIDIRECTIONAL WHEELS

Figure 3 shows a typical omnidirectional wheel. Note that this wheel is slightly different from the continuous alternate wheel (CAW) in structure, but the operational principle is identical. A conventional tire-like wheel possesses 2 DOFs: wheel rotation about the wheel axis on the wheel plane, and rotational slip about the vertical axis passing through the point of contact with the ground. The wheel rotation is conducted by a wheel actuator, while the rotational slip by steering action. An omnidirectional wheel has one more DOF, roller rotation about the roller axis, as shown in Figure 3. Rollers of an omnidirectional wheel are passive since no actuators are used to drive them. Therefore, the passive roller in contact with the ground does not provide any frictional force in the direction normal to the roller axis in free rolling.

The omnidirectional wheel usually has two modes of motion: active rolling and passive rolling. In active rolling a wheel rotates about the wheel axis by a wheel actuator with passive rollers remaining still, while in passive rolling a wheel translates in the direction of the wheel axis with the roller in contact with the ground spinning freely. Motions in other directions involve a combination of wheel rotation and roller rotation. Thus the wheel velocity at the wheel center, V_w, can be decomposed into the active component, V_a, and the passive component, V_p.

There are various types of omnidirectional mobile robots. For instance, some vehicles use three omnidirectional wheels, and others use four wheels to improve vehicle structural stability. Although each different omnidirectional vehicle has its own working operation, the operational steps are similar. A desired vehicle motion is first determined according to the specific task involved. The wheel velocity at each wheel center is then computed to achieve this vehicle motion. The active velocity component for each wheel is then computed and implemented by each wheel actuator. The sign and magnitude of passive velocity component of the passive roller in contact with the ground are automatically determined to satisfy the constraint given by the relationship between the wheel velocity and active velocity components.

3. DESIGN OF PASSIVE ROLLERS

The rollers used in alternate wheels are barrel-shaped as shown in Figure 4, because the surface contour of a roller should match the wheel circumference. Figure 4 shows an alternate wheel with smaller inner rollers and larger outer rollers arranged alternately around it. In each roller, the most convex radius in the middle is termed a center radius, and the radius at its ends is termed an end radius.

The height of a surmountable bump for a universal wheel with passive rollers depends on the minimum roller radius (not on the wheel radius) and friction of a roller.[6] It is preferable, therefore, that the minimum radius of a roller be as large as possible and thus approach the maximum radius for a given wheel size.

3.1. Number and Radii of Rollers

Figure 4 shows configuration of a proposed continuous alternate wheel (CAW) in which the inner and outer rollers alternate. As mentioned previously, the wheel contacts the ground continuously, since

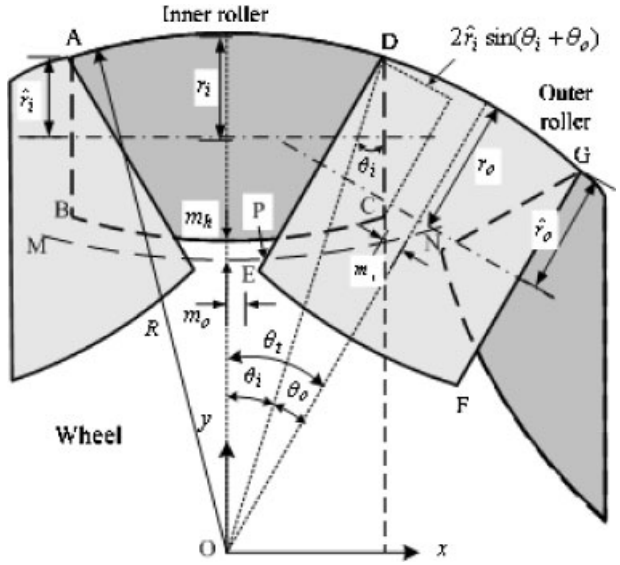

Figure 4. Geometry in continuous alternate wheel.

virtually no gap between rollers exists in this wheel. First, the conditions for no gap between rollers will be investigated below.

From the geometry in Figure 4, the relationship between the wheel radius R and the half-angles θ_i and θ_o for the inner and outer rollers, respectively, becomes

$$2n(\theta_i + \theta_o) = 2\pi, \tag{1}$$

where n represents the number of inner (or outer) rollers. If $n = 4$, for example, the wheel consists of four inner rollers and four outer rollers, and thus $\theta_i + \theta_o$ equals $\pi/4$. The center radius r_i and the end radius $\hat{r}_i$ of an inner roller have the geometric relation

$$r_i = \hat{r}_i + R(1 - \cos\theta_i), \tag{2}$$

and the center radius r_o and the end radius $\hat{r}_o$ of an outer roller have the similar relation

$$r_o = \hat{r}_o + R(1 - \cos\theta_o). \tag{3}$$

Spokes are used to support inner and outer rollers (see Figure 11). The dimensions of a spoke such as width and thickness are determined depending on the maximum load the wheels are subject to. Some space margins between rollers are required for these spokes to be placed. As these margins get larger, fitting the spokes into the rollers gets easier at the cost of a smaller roller radius.

Let m_i be half the margin between inner rollers. Then the end radius of an inner roller for given m_i can be described by

$$(R\sin\theta_o - m_i) \geq 2\hat{r}_i \sin(\theta_i + \theta_o). \tag{4}$$

The end radius of an inner roller for given m_i is then obtained by

$$\hat{r}_i \leq \frac{R\sin\theta_o - m_i}{2\sin(\theta_i + \theta_o)}, \tag{5}$$

and thus the maximum $\hat{r}_i$ becomes

$$\hat{r}_{i\,\max} = \frac{R\sin\theta_o - m_i}{2\sin(\theta_i + \theta_o)}. \tag{6}$$

The maximum r_i is then easily computed by

$$r_{i\,\max} = \hat{r}_{i\,\max} + R(1 - \cos\theta_i). \tag{7}$$

Similarly, the end radius of an outer roller for given m_o is given by

$$\hat{r}_o \leq \frac{R\sin\theta_i - m_o}{2\sin(\theta_i + \theta_o)}, \tag{8}$$

where m_o is half the margin between outer rollers. The maximum end and center radii of an outer roller are then given by

$$\hat{r}_{o\,\max} = \frac{R\sin\theta_i - m_o}{2\sin(\theta_i + \theta_o)}, \tag{9}$$

and

$$r_{o\,\max} = \hat{r}_{o\,\max} + R(1 - \cos\theta_o). \tag{10}$$

As shown in Figure 4, some portion of an inner roller interpenetrates inside of an outer roller. The margin m_h is then needed for some portion of the spoke to reside between surfaces of the inner and outer rollers. The condition for the end radius of an outer roller for the given margin m_h is investigated

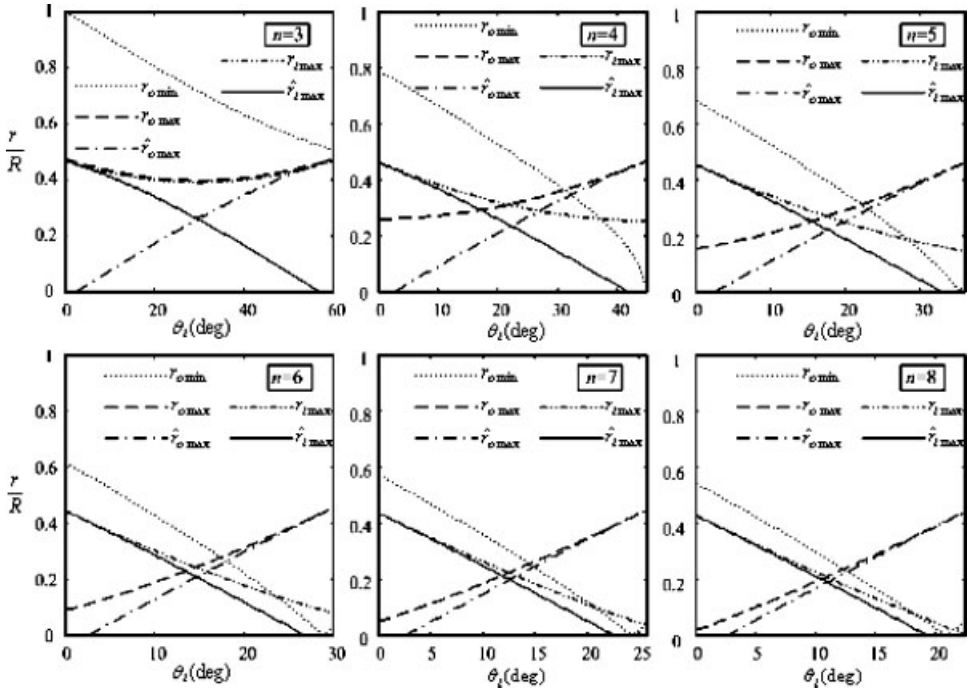

Figure 5. Roller radii as a function of θ_i for various values of n.

below. First, let the xy coordinates be defined at the center of the wheel as shown in Figure 4. The equation for the segment DE is given by

$$y=\frac{1}{\tan(\theta_i+\theta_o)}(x-R\sin\theta_i)+R\cos\theta_i \qquad (11)$$

because the line DE passes the point D whose coordinate is $(R\sin\theta_i, R\cos\theta_i)$ and its slope is $1/\tan(\theta_i+\theta_o)$. The equation of the circle offset by the margin m_h from the surface of the inner roller (represented by the dashed arc MN) is described by

$$x^2+\{y-(2R-2r_i)\}^2=(R+m_h)^2. \qquad (12)$$

Solving Eqs. (11) and (12) yields the intersecting point P whose coordinates are

$$x_P=\frac{-ae\pm\{(a^2+1)f^2-e^2\}^{1/2}}{a^2+1}, \quad y_P=a(x_P-b)+c, \qquad (13)$$

where $a=1/\tan(\theta_i+\theta_o)$, $b=R\sin\theta_i$, $c=R\cos\theta_i$, $d=2R-2r_i$, $e=-ab+c-d$, and $f=R+m_h$.

The segment DP must be less than or equal to the end diameter DE of an outer roller. Hence the minimum end radius of an outer roller is given by

$$\hat{r}_{o\,\min}=\frac{\{(R\sin\theta_i-x_P)^2+(R\cos\theta_i-y_P)^2\}^{1/2}}{2}. \qquad (14)$$

The minimum center radius of an outer roller then becomes

$$r_{o\,\min}=\hat{r}_{o\,\min}+R(1-\cos\theta_o). \qquad (15)$$

In what follows, various design parameters are determined based on the above analysis. First, the margins were determined so that the roller radii become as large as possible by reducing the margins. They were selected as $m_i=5.5$ mm, $m_o=4.5$ mm, and $m_h=7.0$ mm for the wheel with a radius of $R=10$ cm in the actual design.

Given a wheel radius R and the margins m_i, m_o, and m_h, the maximum and minimum radii of the inner and outer rollers can be determined as a function of θ_i (or, equivalently, θ_o) and n. Based on Eqs. (6), (7), (9), (10), and (15), the roller radii as a function of θ_i for $n=3$–8 are illustrated in Figure 5. In the figure, the maximum radius of an outer roller should be searched for in the region of $r_{o\,\max}\geq r_{o\,\min}$; otherwise, no solution exists. It is found that there is no solution for $n=3$, since $r_{o\,\min}$ is greater than $r_{o\,\max}$ in the entire

Table I. Comparison of design parameters for various alternate wheels.

Parameters	ref. 7	CAW	ref. 9	CAW
n	4	4	6	6
R	10 cm	10 cm	10 cm	10 cm
θ_i	42.3°	31.2°	18.2°	17.4°
θ_o	12.7°	13.8°	11.8°	12.6°
ϕ	⋯	65.6°	⋯	65.7°
r_o	24.0 mm	36.3 mm	22.5 mm	27.8 mm
$\hat{r}_o$	16.5 mm	33.4 mm	19.5 mm	25.4 mm
r_i	12.0 mm	27.4 mm	15.0 mm	20.9 mm
$\hat{r}_i$	4.5 mm	12.9 mm	9.0 mm	16.3 mm

range of θ_i. It is observed that as θ_i increases, the radii of the outer roller increase, but those of the inner roller decrease. Therefore, the maximum end radius of the inner roller $\hat{r}_{i\,\max}$ corresponds to the point where $r_{o\,\max}=r_{o\,\min}$ in the plots. Equating Eq. (10) to (15) yields

$$\frac{\{(R\sin\theta_i-x_P)^2+(R\cos\theta_i-y_P)^2\}^{1/2}}{2}=\frac{R\sin\theta_i-m_o}{2\sin(\theta_i+\theta_o)}. \tag{16}$$

Since this equation cannot be solved explicitly, the numerical solution is obtained.

Table I compares the cases ($n=4$ and 6) designed by the proposed method with those of refs. 7 and 8. The roller radii increase by 150%–280% for $n=4$ and 120%–180% for $n=6$ for the same wheel radius. Figure 6 shows the roller radii as a function of n. It is noted from the figure that for $n<6$, the end radius of an inner roller gets smaller while the other radii get larger. For $n>6$, all the radii tend to decrease, which is not desirable from the viewpoint of the height of a surmountable bump. Considering all these facts, the number of rollers was chosen as six in the design of a continuous alternate wheel. It is noted that the roller radii are maximized for given margins between rollers, and the inner and outer rollers are connected continuously along the wheel circumference.

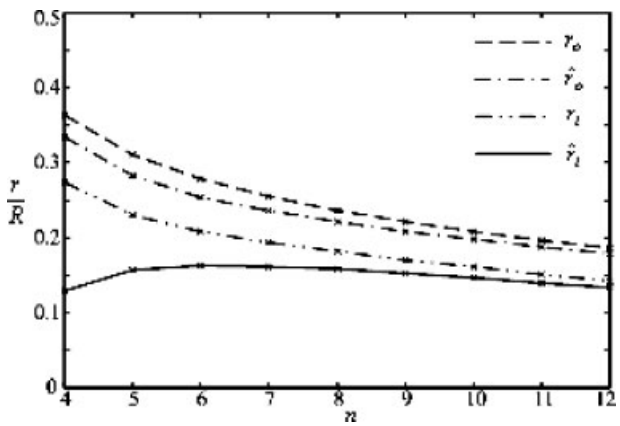

Figure 6. Variation of radii of inner and outer rollers as a function of n.

3.2. Interior Shape of Outer Roller

The structure of a continuous alternate wheel involves slight interpenetration of the inner roller into the interior of an outer roller. Therefore, an empty space must be on the interior of the outer roller to avoid interference with inner roller. This space should include the solid of revolution which is cut out by the side circle of an inner roller (imagine the edge of a knife is on the circumference of the side circle) inside an outer roller when the outer roller rotates about its axis as shown in Figure 7.

The side circle of an inner roller whose diameter is CD can be found by the intersection of the sphere

$$(x-\hat{r}_i\sin\theta_t)^2+(y-\hat{r}_o+\hat{r}_i\cos\theta_t)^2+z^2=\hat{r}_i^2 \tag{17}$$

and the plane

$$y=-x/\tan\theta_t+\hat{r}_o. \tag{18}$$

The distance L between a point on the circumference of the side circle of an inner roller and the x-axis which is the rotational axis of an outer roller is expressed by

$$L(x)^2=y^2+z^2. \tag{19}$$

Substituting Eqs. (17) and (18) into (19) yields

$$L(x)=\left(\hat{r}_o^2-x^2-2\left(\frac{\hat{r}_o\cos\theta_t-\hat{r}_i}{\sin\theta_t}\right)x\right)^{1/2}. \tag{20}$$

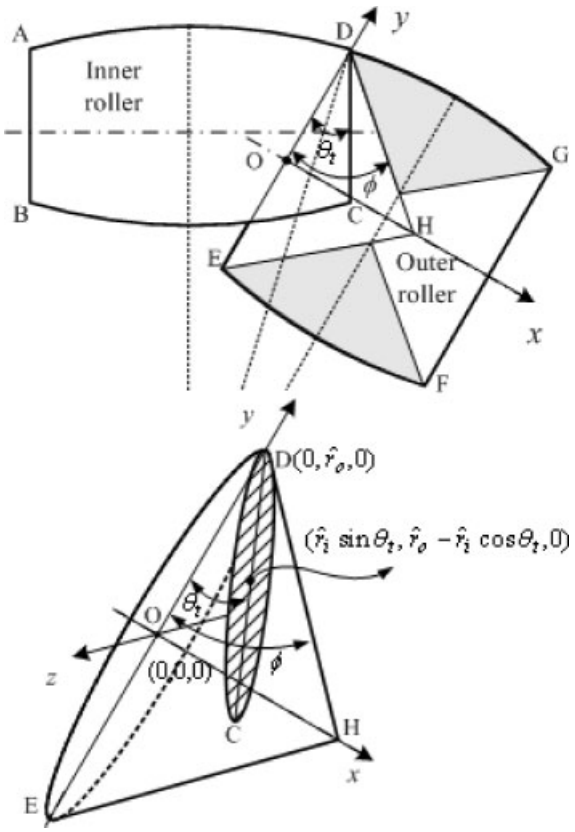

Figure 7. Interpenetration of inner roller into outer roller.

Figure 8 shows the projected trajectory of $L(x)$ onto the xy plane. For the convenience of fabrication, the inside shape of an outer roller is chosen as a circular cone whose vertex is the point H. The design parameter of this cone is the inclination angle ϕ in Figure 8. As ϕ decreases, the fringe of an outer roller can be thicker, thus leading to more solid structure. It is desirable, therefore, that ϕ be as small as possible unless any interference between rollers occurs. Since the minimum value of ϕ happens to be the slope of $L(x)$ at $x=0$, it can be found by differentiation of Eq. (20) with respect to x

$$\frac{dL(x)}{dx} = -\frac{x + (\hat{r}_o \cos\theta_t - \hat{r}_i)/\sin\theta_t}{\{\hat{r}_o^2 - x^2 - 2[(\hat{r}_o \cos\theta_t - \hat{r}_i)/\sin\theta_t]x\}^{1/2}}. \tag{21}$$

Hence

$$\left.\frac{dL(x)}{dx}\right|_{x=0} = -\frac{1}{\hat{r}_o}\frac{\hat{r}_o \cos\theta_t - \hat{r}_i}{\sin\theta_t} = \frac{\hat{r}_i/\hat{r}_o - \cos\theta_t}{\sin\theta_t}$$
$$= -1/\tan\phi_{\min}, \tag{22}$$

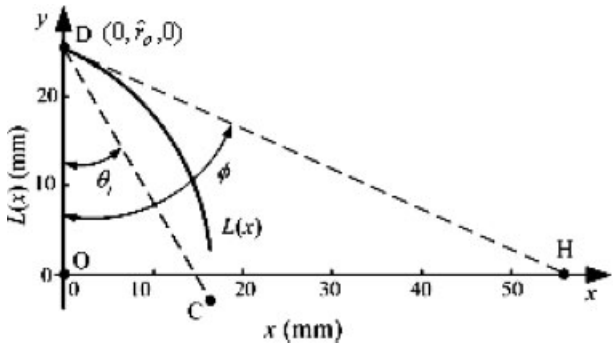

Figure 8. Function $L(x)$ representing distance between points on side circle of inner roller and rotational axis of outer roller.

and the minimum inclination angle is obtained by

$$\phi_{\min} = \tan^{-1}\left(\frac{\sin\theta_t}{\cos\theta_t - \hat{r}_i/\hat{r}_o}\right). \tag{23}$$

Note that the angle ϕ in Table I was computed by Eq. (23).

4. CONSTRUCTION AND TESTS OF CONTINUOUS ALTERNATE WHEELS

4.1. Construction of CAW

An actual continuous alternate wheel was constructed based on the design parameters given in Table I ($n=6$). The important dimensions of the wheel are shown in Figure 9. In the process of construction, more design factors other than the previously determined ones such as the number of rollers, roller radii, and the interior inclination angle of an

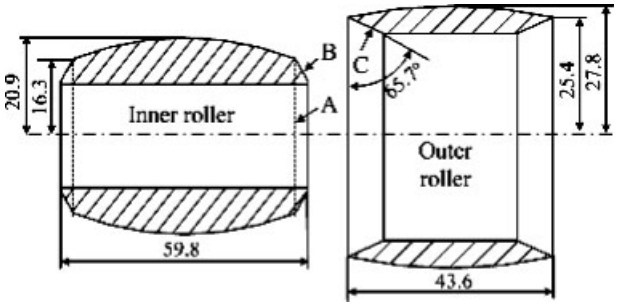

Figure 9. Final shapes of inner and outer rollers.

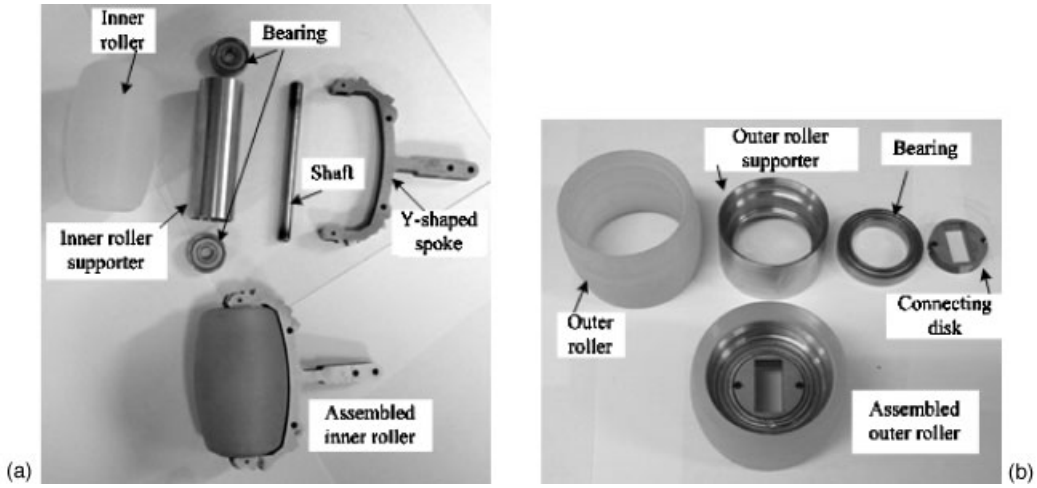

Figure 10. Photo of roller parts and assembled rollers; (a) parts of inner roller and (b) parts of outer roller.

outer roller were considered. This section is concerned with the overall structure of a continuous alternate wheel.

The shapes of inner and outer rollers designed in the previous section are capable of continuously contacting the ground without any interference between rollers. Polyurethane was selected as the roller material since it provides an appropriate friction coefficient and mechanical properties suited to an omnidirectional wheel. However, a urethane roller is not solid enough to prevent deformation when it is subject to loads due to contact with the ground. Therefore, steel supporters in the form of a hollow cylinder are inserted into the rollers to support urethane rollers.

Referring to Figure 8, the fringe of the outer roller is relatively thin to avoid interference with the inner roller. This thin fringe, however, cannot be supported by any supporter, since the supporter may interfere with the inner roller. As a result, the thin fringe of the outer roller is not solid enough to bear the external load due to contact with the ground. To overcome this problem, the final shape of the rollers is designed as shown in Figure 9. The inside surface of an outer roller forms a circular cone (denoted C in Figure 9) with the inclination angle determined by the previous analysis. Note that another circular cone (denoted B) is added to the original sides of the inner roller (denoted A). These circular cones B and C do not contact each other when no external load is exerted on the wheel, since a small margin exists between the two surfaces. When the thin portion of the outer roller makes contact with the ground, however, surface C is pressed against surface B. Then, surface B supports surface C, and actually they rotate together about each roller axis. In this way, the problem of deformation of the fringe of an outer roller can be overcome without causing any interference with the inner roller.

A supporting structure is required to hold rollers around the wheel. The supporting parts for the inner roller are composed of a supporter, bearings, a shaft, and a spoke, while those for the outer roller consist of a supporter, a bearing, and a connecting disk as shown in Figure 10. Figure 11 shows a schematic diagram and a cutaway view of the final wheel and

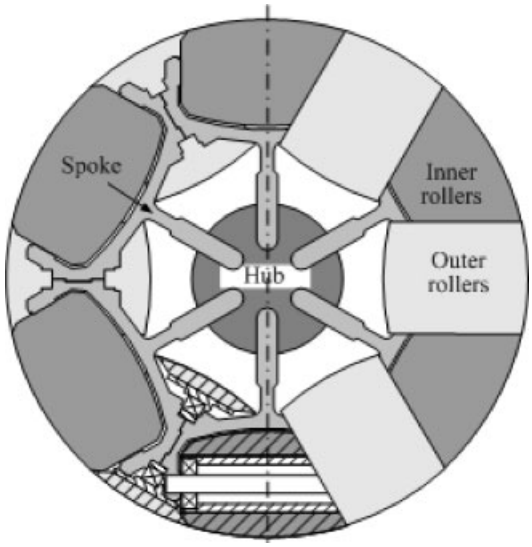

Figure 11. Schematic diagram of proposed continuous alternate wheel.

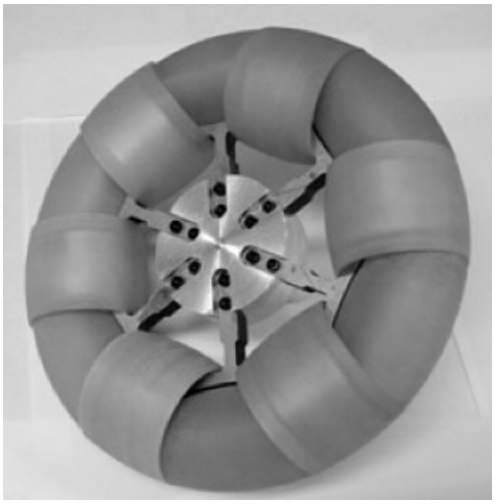

Figure 12. Photo of constructed continuous alternate wheel.

Figure 12 is a photo of the finally assembled continuous alternate wheel. As shown in Figure 11, the wheel has a hub with radially disposed six Y-shaped spokes made of stainless steel. Each spoke supports one inner roller through the roller axis with bearings at both ends. Two successive spokes, on the other hand, support the outer roller together through bearings.

The total weight of a wheel is about 2.5 kg. The payload of the omnidirectional robot with proposed wheels is about 100 kg because it is designed to carry one person on it. Since the robot body weighs 49 kg including four wheels, each wheel is designed to carry a vertical load of 50 kg. FEM analysis was carried out to investigate deformation and strength of the wheel at the design stage of the wheel. Deformation and stress distributions for three parts—the inner roller, the overlap of the inner and outer rollers, and the outer roller—in contact with the ground were computed by the I-DEAS package while the wheel subject to a vertical load of 50 kg rolls on the ground. Figure 13 shows the stress distribution of the inner roller. From these distributions, the maximum deformations and stresses were found and listed in Table II. A maximum deformation of 2.30 mm occurs at the polyurethane of the outer roller. A maximum stress occurs at the supporter of the outer roller, but its value of 14.8 MN/m^2 is far smaller than the yield strength of stainless steel (e.g., 200 MN/m^2). It follows from the FEM analysis that the designed wheels provide sufficient strength to carry the payload of 100 kg. Actually, no problems have been found in the various tests in which an operator of the vehicle sits on the vehicle during its operation.

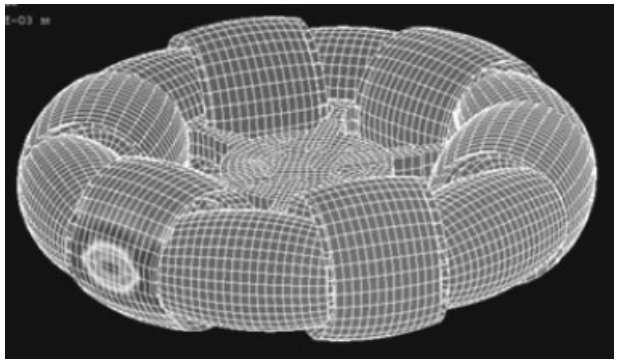

Figure 13. Stress distribution of inner roller of wheel subject to a vertical load of 50 kg.

4.2. Tests

It is not easy to evaluate wheel performance during motion since it is impractical to place sensors on the passive rollers to measure their behavior. Because the CAWs are meaningful only when used in an omnidirectional vehicle, a prototype omnidirectional vehicle with four wheels shown in Figure 14 has been built.[9] Each wheel module is composed of a CAW and a wheel motor. Since only 3 DOFs are required in an omnidirectional motion on the plane, 1 DOF is redundant and thus used for steering. Four wheel modules can steer about each pivot point located at the corners of the vehicle body, but they are constrained to have a synchronized steering motion of 1 DOF (i.e., identical magnitudes of all four steering angles) by the synchronous mechanism comprising a linear guide and connecting links. In summary, a combination of four independent control of wheels generates an omnidirectional motion.

Some performance tests for the prototype vehicle have been conducted. Tracking performance of the

Table II. Maximum deformations and stresses for various parts of the wheel.

Parts	Maximum deformation (mm)	Maximum stress (MN/m^2)
Inner roller	1.99	7.78
Overlap of two rollers	1.40	4.73
Outer roller	2.30	14.8

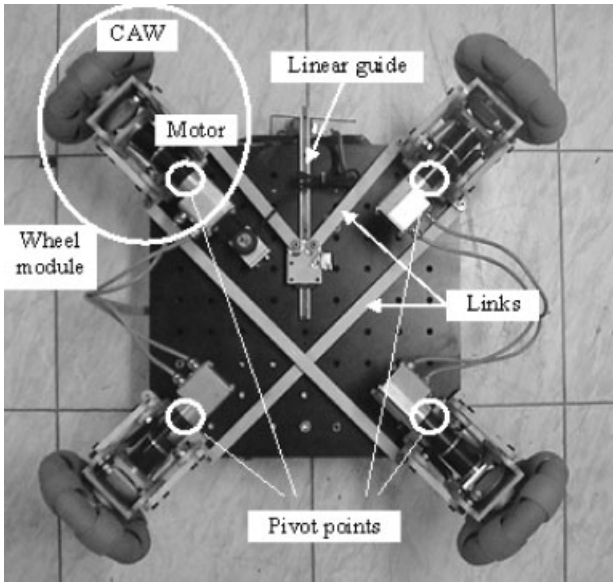

Figure 14. Bottom view of prototype vehicle with CAWs.

vehicle with one person on it has been tested for various trajectories. Given a circular reference trajectory represented in the dashed line in Figure 15, the vehicle control algorithm generates the required vehicle velocity and then computes the velocity of each wheel to achieve the desired motion through the Jacobian analysis. In the figure, the triangle indicates the position and orientation of a vehicle. The vehicle front is always directed toward the center of a circular path during motion, which is not feasible in the conventional vehicles. It is seen that the actual trajectory represented in the solid line tracks the reference reasonably well. Some error is observed around the finish since the prototype vehicle does not implement any position control algorithm for this test and thus position error has been accumulated during motion.

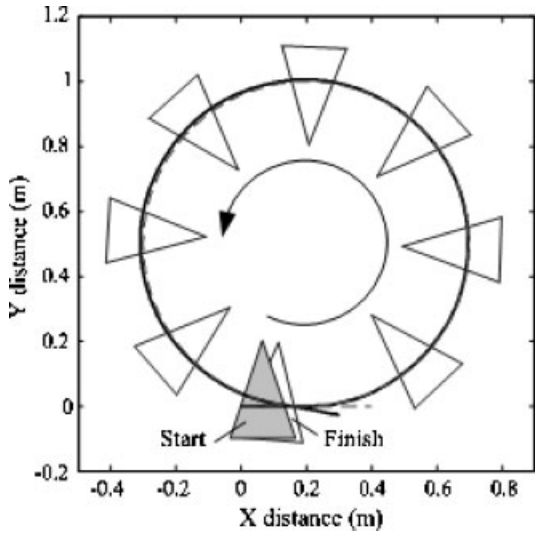

Figure 15. Experimental results of tracking performance for a circular trajectory (solid line: actual trajectory, dashed line: reference trajectory).

5. CONCLUSION

In this research a new design of a continuous alternate wheel (CAW) was proposed to minimize a gap between rollers and to maximize radii of rollers. The gap causes vertical and/or horizontal vibrations in many types of omnidirectional wheels with passive rollers, and roller radii are related to the height of a surmountable bump. This wheel is an improved version of a conventional alternate wheel where inner and outer rollers are disposed alternately.

This paper details the systematic design procedure of the continuous alternate wheel. That is, the design guidelines were presented to determine the optimum number of rollers, the radii of rollers, and the inside inclination angle of an outer roller for given design specifications. It is shown that the proposed continuous alternate wheel can provide larger radii of the roller for the same size of the wheel than already existing alternate wheels.

Using the polyurethane rollers, the actual continuous alternate wheel was constructed to verify validity of the design guidelines. The omnidirectional mobile robots equipped with these proposed wheels were built and their tracking performance for various trajectories was evaluated.

REFERENCES

1. M. Wada and S. Mory, Holonomic and omnidirectional vehicle with conventional tires, Int Conf on Robotics and Automation, 1996, pp. 3671–3676.
2. M. West and H. Asada, Design of ball wheel mechanisms for omnidirectional vehicles with full mobility and invariant kinematics, J Mech Des 119 (1997), 153–161.
3. J.F. Blumrich, Omnidirectional vehicle, United States Patent 3,789,947, 1974.
4. B.E. Ilou, Wheels for a course stable self-propelling vehicle movable in any desired direction on the ground or some other base, United States Patent 3,876,255, 1975.
5. H. Asada, M. Sato, and L. Bogoni, Holonomic and omnidirectional vehicle with conventional tires, Int Conf on Robotics and Automation, 1995, pp. 1925–1930.
6. L. Ferriere, B. Raucent, and G. Campion, Design of

omni-mobile robot wheels, Int Conf on Robotics and Automation, 1996, pp. 3664–3670.
7. C. Fuchs, The wheel that enables to move immediately in every direction, Germany Patent 822,660, 1951.
8. H. Asama, M. Sato, N. Goto, A. Matsumoto, and I. Endo, Mutual transportation of cooperative mobile robots using forklift mechanisms, Int Conf on Robotics and Automation, 1996, pp. 1754–1759.
9. K.-S. Byun, S.-J. Kim, and J.-B. Song, Design of a four-wheeled omnidirectional mobile robot with variable wheel arrangement mechanism, Int. Conf. on Robotics and Automation, 2002, pp. 720–725.